

## Efficient generation of graph states for quantum computation

**S R Clark<sup>1,3</sup>, C Moura Alves<sup>1,2</sup> and D Jaksch<sup>1</sup>**

<sup>1</sup> Clarendon Laboratory, University of Oxford, Parks Road,  
Oxford OX1 3PU, UK

<sup>2</sup> DAMTP, University of Cambridge, Wilberforce Road,  
Cambridge CB3 0WA, UK

E-mail: [s.clark@physics.ox.ac.uk](mailto:s.clark@physics.ox.ac.uk)

*New Journal of Physics* **7** (2005) 124

Received 28 February 2005

Published 18 May 2005

Online at <http://www.njp.org/>

doi:10.1088/1367-2630/7/1/124

**Abstract.** We present an entanglement generation scheme which allows arbitrary graph states to be efficiently created in a linear quantum register via an auxiliary entangling bus (EB). The dynamical evolution of the EB is described by an effective non-interacting fermionic system undergoing mirror-inversion in which qubits, encoded as local fermionic modes, become entangled purely by Fermi statistics. We discuss a possible implementation using two species of neutral atoms stored in an optical lattice and find that the scheme is realistic in its requirements even in the presence of noise.

<sup>3</sup> Author to whom any correspondence should be addressed.

**Contents**

<b>1. Introduction</b>	<b>2</b>
<b>2. Non-interacting fermionic system</b>	<b>4</b>
2.1. Mirror inversion on a lattice . . . . .	4
2.2. Entanglement of fermionic modes . . . . .	5
2.3. Generalizations . . . . .	6
<b>3. Entanglement generation scheme</b>	<b>6</b>
<b>4. Implementations</b>	<b>7</b>
4.1. Optical lattice realization . . . . .	7
4.2. Optical lattice imperfections . . . . .	9
4.3. Alternative implementations . . . . .	10
<b>5. Conclusions</b>	<b>10</b>
<b>Acknowledgments</b>	<b>11</b>
<b>References</b>	<b>11</b>

**1. Introduction**

Bipartite entanglement has long been recognized as a useful physical resource for tasks such as quantum cryptography and quantum teleportation. Similarly, multipartite entanglement is an essential ingredient for more complex quantum information processing (QIP) tasks, and interest in this resource has grown since its controlled generation was demonstrated in several physical systems [1]–[5]. An important class of multipartite entangled states are graph states. By using vertices in a graph to represent qubits, and edges to represent an Ising-type interaction that has taken place between two qubits, the graph formalism gives an intuitive characterization of entanglement by the presence of edges [6]. As a result, a graph represents a preparation procedure for a state. Additionally, graph theory allows some properties of these states, such as the effects of local Pauli operations and the persistence of entanglement after local Pauli measurements, to be computed exactly, and others, such as the Schmidt measure, which is computationally intractable for general states, to be bounded from above and below [6, 7]. The class of graph states includes many well-studied states such as GHZ states, and special instances of graph states are the resources used in quantum error correcting codes [8, 9] and in one-way quantum computing [10, 11].

Initial proposals for the generation of graph states in physical systems have focused on qubit lattices of fixed geometry, where each qubit interacts only with its nearest-neighbours [6, 7, 11]. Such a scheme has been experimentally implemented in a three-dimensional (3D) optical lattice of neutral atoms via controlled collisions [1] along one axis of the lattice. The graph states generated with this method follow the geometry of the lattice, and so for collisions along one axis an array of 1D cluster states, similar to figure 1(a), was obtained. Extending this process to all axes of 2D and 3D square lattices, generates cluster states of the form shown in figures 1(b) and (c) respectively. These both constitute, together with single-qubit measurements, a universal resource for quantum computation [10]. Despite the 1D cluster states of the type shown in figure 1(a) not being a universal resource, they are still a useful resource for specific computational

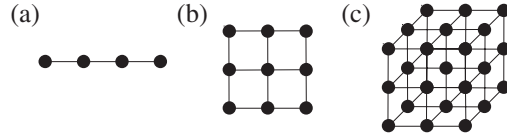


**Figure 1.** Examples of (a) 1D, (b) 2D and (c) 3D cluster states. States (b) and (c) (and larger versions thereof) are a universal resource for one-way quantum computing.

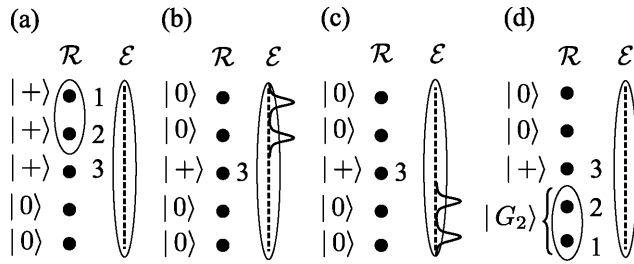


**Figure 2.** (a) Consider a quantum register  $\mathcal{R}$  which has three graph qubits in a state  $|+\rangle$ . (b) Two of them are transferred to the EB  $\mathcal{E}$  where their state is mapped into local fermionic modes (LFMs). (c)  $\mathcal{E}$  evolves via  $H_f$  for time  $\tau$ , which results in the mirror-inversion of the two qubits. (d) The qubits at the mirror-inverted location are transferred back to  $\mathcal{R}$ , yielding a graph state with two vertices  $|G_2\rangle$ . Repeating this procedure with different qubits allows any 3-qubit graph state to be generated in  $\mathcal{R}$ .

tasks, as emphasized by the recent use of the four-qubit 1D cluster state to implement the two-qubit Grover search algorithm with photons [3]. More generally, wider classes of graph states also represent specific resources for certain QIP tasks, and this builds upon the notion that entanglement is an algorithmic resource [11]. The direct generation of arbitrary graphs, where the set of edges does not translate into a regular arrangement of the underlying qubits, e.g. the quantum Fourier transform graph state [6], requires the ability to pre-engineer a complicated geometry of the qubit interactions. A simple scheme in which any graph state can be created in a set of qubits with a regular fixed geometry is therefore highly desirable. Some progress has been made towards this with non-deterministic linear optical protocols, where proposals have been made for graph state generation in photon [12] and solid-state qubits [13].

In this paper, we propose a deterministic scheme for efficiently generating arbitrary graph states within a linear quantum register. We consider a general setup in which there is an auxiliary system, denoted as an entangling bus (EB), running parallel and along the length of the register. All entanglement within the register is generated via the EB by performing local swaps between subsets of register qubits and the EB and allowing the EB to evolve for a fixed time. More specifically, the EB is an ‘always on’ 1D system whose dynamical evolution over a fixed time generates a specific entangling operation  $\mathcal{C}$  composed of controlled- $\sigma_z$  ( $c\text{-}\sigma_z$ ) gates between all pairs of the transferred qubits in one step. After local swaps back to the register, this operation can generate GHZ-type graph states [6] within this subset of register qubits. Repeated use of this entangling operation then allows arbitrary graph states to be generated in the register, as depicted for the simplest case with two qubits in figure 2. This setup is motivated by the following three results.

Our first result is a construction of the EB using a system which maps onto a 1D non-interacting fermionic lattice. Within this mapping, qubits from the register become encoded as local fermionic modes (LFMs) [14]. We begin in section 2 by showing that, for an engineered lattice with a specific spatially varying hopping profile, the dynamical evolution over some fixed time results in the complete mirror-inversion of the LFMs. This inversion is then shown to generate robust phases within the fermionic state purely as a consequence of Fermi statistics which are equivalent to entanglement between the LFM qubits resulting from an effective entangling operation  $\mathcal{C}$ .

Our second result described in section 3 is then a scheme which utilizes the availability of the entangling operation  $\mathcal{C}$  through the EB to efficiently generate arbitrary graph states within the register. Specifically, we show that any graph state of  $n$  vertices can be generated in at most  $O(2n)$  EB steps representing an improvement over the  $O(n^2)$  steps required in a network model composed of two-qubit gates.

In section 4 we present our third result which is a proposal for the implementation of this scheme in an optical lattice of neutral atoms. We begin by examining how an effective  $XY$  spin chain can be engineered within an optical lattice. Two adjacent spin chains then form the basis of the register and EB. We investigate how imperfections in the mapping of the optical lattice to an  $XY$  spin chain alter the fidelity of the EB dynamics. Finally, we briefly note some other viable alternatives for implementing this scheme, and conclusions are given in section 5.

## 2. Non-interacting fermionic system

### 2.1. Mirror inversion on a lattice

The construction of the fermionic EB relies on the fermionic system being mapped from another underlying system. The specific example we considered is an  $XY$  spin chain composed of  $N$  spins which is described by the Hamiltonian

$$H_{xy} = \sum_{n=1}^N \lambda_n^z \sigma_n^z - \sum_{n=1}^{N-1} \lambda_n^{xy} (\sigma_n^x \sigma_{n+1}^x + \sigma_n^y \sigma_{n+1}^y), \quad (1)$$

where  $\lambda_n^{xy}$  are the spatially varying  $XY$  couplings and  $\lambda_n^z$  is the contribution of an external field taken to be uniform as  $\lambda_n^z = B/2$ . It is well known that the Jordan Wigner transformation (JWT) [15] maps the  $XY$  spin chain to a non-interacting fermionic Hamiltonian

$$H_f = \sum_{n=1}^N u_n c_n^\dagger c_n - \sum_{n=1}^{N-1} j_n (c_n^\dagger c_{n+1} + c_{n+1}^\dagger c_n), \quad (2)$$

where  $j_n = 2\lambda_n^{xy}$ ,  $u_n = B$  and  $c_n$  is a fermionic destruction operator for the  $n$ th site obeying the usual anticommutation relations. We are particularly interested in the angular momentum hopping profile [16] given by  $j_n = (J/2)\sqrt{n(N-n)}$ , with  $J$  a constant. We choose to write this as  $j_n = W\alpha_n$  with  $\alpha_n = 2\sqrt{(n/N)[1-(n/N)]}$  and  $W = JN/4$ . In this way, the spatial dependence of the hopping  $j_n$  is contained entirely in the profile  $\alpha_n$  obeying  $0 < \alpha_n \leq 1$ , and the overall scaling is given by the constant  $W$  such that  $\max(j_n) \leq W$ . With this hopping profile, the projection of  $H_f$  onto the single fermion subspace of the lattice,  $\mathcal{H}_1$ , results in a Hamiltonian

equivalent to  $H_1 = -JS_x + B1$ , where  $S_x$  is the  $x$ -angular momentum operator for an ‘effective’ spin- $S$  particle, with  $S = (N - 1)/2$ . The single-fermion states  $\{|n\rangle = c_n^\dagger |\text{vac}\rangle\}$  then correspond to the  $z$ -angular momentum eigenstates  $\{|S, l\rangle_z\}$  of the spin- $S$  particle, with  $|1\rangle = |S, -S\rangle_z, \dots, |N\rangle = |S, S\rangle_z$ . The dynamical evolution generated in  $\mathcal{H}_1$ , when  $H_1$  is applied for a fixed time  $\tau = \pi/J$ , result in the unitary time-evolution operator  $U_1(\tau) = \exp(i\phi_B) \exp(i\pi S_x)$  composed of an overall phase  $\phi_B = -B\pi/J$  for  $\mathcal{H}_1$  and a rotation of the spin- $S$  particle about the  $x$ -axis by  $\pi$ . This leads directly to perfect state transfer over the lattice [16].

The action of  $U_1(\tau)$  on the single-particle basis follows from its equivalence to the  $z$ -angular momentum states where  $\exp(i\pi S_x) |S, l\rangle_z = \exp(i\pi S) |S, -l\rangle_z$ . Thus we find that  $U_1(\tau) |n\rangle = \exp(i\phi_1) |\bar{n}\rangle$ , with the phase  $\phi_1 = \pi S + \phi_B$  and mirror-conjugate location  $\bar{n} = N - n + 1$ . The choice  $B = SJ$  then ensures that the single-particle phase  $\phi_1$  vanishes. The evolution of the fermionic modes  $c_n^\dagger$  can then immediately be seen to satisfy  $U c_n^\dagger U^\dagger = c_{\bar{n}}^\dagger$ , where  $U = \exp(-iH_f\tau)$ , with respect to the full Hamiltonian  $H_f$ , and the dynamical evolution of the system describes the complete mirror-inversion of the LFMs. Typically, implementations of this effective fermionic system will have a maximum obtainable value for the overall scaling  $W$  of the hopping which prevents  $J$  from being arbitrarily increased, and so once it is maximized we must pay a linear cost in the inversion time  $\tau$  with the increasing size of the system  $N$ .

## 2.2. Entanglement of fermionic modes

Under the JWT, the  $N$  qubit (or spin) states  $|q_1, \dots, q_N\rangle$ , with  $q_n \in \{0, 1\}$ , of the chain are mapped onto Fock states of the LFMs as  $|q_1, \dots, q_N\rangle = (c_1^\dagger)^{q_1} \dots (c_N^\dagger)^{q_N} |\text{vac}\rangle$  (where operators are ordered according to the lattice), which describe the occupancy of the system by quasi-fermions. The use of fermionic mode occupancy as a basis for quantum computation has been proposed before [14]. An immediate difficulty with a direct implementation of this approach using massive and/or charged fermions is the constraint caused by superselection rules, which prohibits the superposition of states with different mass/charge eigenvalues [17, 18]. Such superpositions are essential for encoding qubits as LFMs. In [14] the accessibility of the Fock space is widened by including an interaction with a superconducting reservoir that relaxes particle number conservation to modulo 2 via the exchange of Cooper pairs. Also, in contrast to bosons, the Fock space of fermions does not have a natural tensor product structure permitting independent operations on each mode [19]. This intrinsically non-local behaviour of fermions adds a significant degree of complexity to quantum computing with LFM qubits in [14]. Here, in contrast, we have focused on a physical system which maps onto a non-interacting fermionic system. As a result, the quasi-Fock space is fully accessible, thus enabling superpositions of states with different numbers of quasi-fermions, which are essential for encoding qubits.

For systems of identical fermions, a bilinear fermionic Hamiltonian such as  $H_f$  suffices to generate mode entanglement, despite describing a non-interacting system [20]. This is a natural consequence of the non-local character of fermions. The entanglement generated by mirror-inversion then follows straightforwardly from Fermi statistics through its action on Fock states as

$$e^{-iH_f\tau} |q_1, \dots, q_N\rangle = e^{-i\pi \sum_Q} |q_N, \dots, q_1\rangle, \quad (3)$$

where  $\sum_Q$  is the number of anticommutations of the operators  $c_n^\dagger$  required to reestablish a Fock state. Specifically,  $\sum_Q = Q(Q - 1)/2$ , where  $Q$  is the number of fermions, i.e.

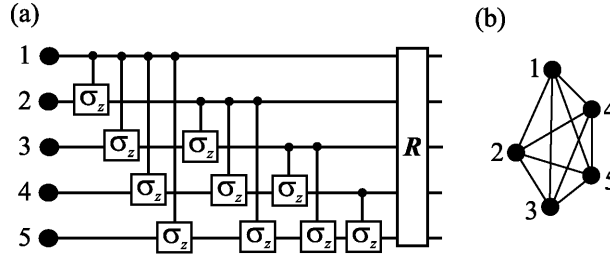


**Figure 3.** For five qubits we have (a) the quantum circuit  $\mathcal{C}(5)$  equivalent to the dynamics of  $H_f$  for a time  $\tau$ , and (b) the fully connected graph state  $|G_5\rangle$  with five vertices generated by this circuit if all the qubits are initialized in the  $|+\rangle$  state. Both the circuit and the resulting graph state generalize in an obvious way for more qubits.

$Q = \sum_{n=1}^N c_n^\dagger c_n = \sum_{n=1}^N q_n$ , and so phases are only acquired between subspaces with different  $Q$ . Since equation (3) is written in terms of Fock states, the inverse-JWT removes the implicit antisymmetry when mapping back to qubits, while leaving the phases acquired between fermion-number (or total magnetization) subspaces untouched. Thus the evolution of the EB after a fixed time  $\tau$  is equivalent to a quantum circuit  $\mathcal{C}(N)$  composed of  $c\text{-}\sigma_z$  gates between all distinct pairs of  $N$  qubits followed by the inversion operator  $R$ , as shown in figure 3(a) for  $N = 5$ . Usefully, if any  $N - q$  qubits of the system are in the state  $|0\rangle$ , then this circuit reduces to  $\mathcal{C}(q)$  between the remaining  $q$  qubits, independent of their locations, followed by the full inversion  $R$  of all qubits.

### 2.3. Generalizations

In passing we note that the above results apply to more general settings. Suppose we partition the fermionic lattice into  $M$  equal blocks, each labelled by their central site  $k$ , and composed of sites  $m(k)$ . Within each block  $k$ , we consider an extended fermionic mode  $f_k^\dagger = \sum_{n \in m(k)} \phi_n^k c_n^\dagger$ , defined by a single-particle state  $\phi_n^k$  contained entirely within the block  $k$  and symmetrical about its centre. The dynamics of the EB over some fixed time will be equivalent to  $\mathcal{C}(M)R$ , as long as  $j_n$  and  $u_n$  are chosen such that the dynamics of  $H_f$  performs mirror-inversion with respect to the modes  $f_k^\dagger$  [21, 22]. We can equally consider partitioning a 1D continuous fermionic system, described by field operators  $\hat{\psi}^\dagger(x)$ , and defining extended LFMs analogously as  $f_k^\dagger = \int_{m(k)} dx \phi^k(x) \hat{\psi}^\dagger(x)$ , via a single-particle wavefunction  $\phi^k(x) = 0, \forall x \notin m(k)$ . In this case, harmonic trapping  $V(x) = m\omega^2 x^2/2$  and Gaussian wavefunctions  $\phi^k(x)$  centred on a block are sufficient for mirror-inversion over a time  $\tau = \pi/\omega$ . Such an arrangement could potentially be implemented using effective bosonic Fock states of arrays of atomic quantum dots [23], following conceptually similar lines to the 1D cold-collision proposal in [24], but with the difference that the Tonks–Girardeau limit [25] of the bosons is exploited to yield robust phases from an effective non-interacting fermionic system.

## 3. Entanglement generation scheme

To generate arbitrary graph states within a linear register of  $N$  storage qubits, we utilize the entangling operation  $\mathcal{C}$  implemented by the EB repeatedly. As with other such schemes, each



qubit in the register is assumed to be individually manipulable and measurable. This includes the ability for each qubit to be selected to undergo a transfer process which maps its state into an LFM-encoded qubit in the EB, via  $\sigma_n^+ \mapsto c_n^\dagger$ , where  $\sigma_n^+$  is the Pauli ladder operator on the register. Since the register is a distinct commuting physical system to the EB the transfer process allows certain sets of qubits to be temporarily endowed with fermionic character and subsequently become entangled as a result of the mirror-inversion of the fermionic modes.

The register and the EB are taken to be initialized in the states  $\bigotimes_i^N |0\rangle_i$  and  $|\text{vac}\rangle$  respectively. The scheme begins by choosing a set of register qubits  $\Gamma$  to be the graph vertices, and applying a Hadamard transformation to each of them:  $|0\rangle \rightarrow |+\rangle = (|0\rangle + |1\rangle)/\sqrt{2}$ , as in figure 2(a) for qubits 1–3. A subset  $\Sigma$  of  $m$  of these qubits is then transferred to the EB and allowed to evolve for a time  $\tau$ , as shown (for  $m = 2$ ) in figure 2(b) and (c) for qubits 1 and 2. The qubits encoded by LFMs at the corresponding mirror-inverted locations  $\bar{\Sigma}$  of the EB are then transferred back to the register, yielding a fully connected graph state  $|G_m\rangle$  between these  $m$  vertices, as in figure 2(d). Such a state is locally equivalent to an  $m$ -qubit GHZ state, as depicted in figure 3(b) for  $m = 5$ . Overlap between EB and register graph qubits after inversion can be avoided by choosing  $|\Gamma| = \lceil N/2 \rceil$  with locations in the first half of the register.

This setup can generate any graph state of  $n$  vertices in at most  $O(n^2)$  steps by utilizing only the two-qubit interaction of the EB to establish each edge individually, mimicking a network model of two-qubit gates. However, by exploiting the multiqubit circuit  $\mathcal{C}$  implemented by the EB dynamics over the same time  $\tau$ , as in figure 3(a), our scheme can improve this upper bound. Specifically, we proceed iteratively, starting with  $g = 1$ , by

- (1) transferring the  $g$ th graph qubit, and all graph qubits  $g_c > g$  which will connect to  $g$ , into the EB;
- (2) allowing them to evolve for a time  $\tau$  creating a complete set of connections between these vertices, cf figure 3(b);
- (3) then transferring qubit  $g$  back to the register while leaving the qubits  $g_c$  to evolve for one cycle longer in the EB, subsequently removing all the connections between them;
- (4) finally transferring the qubits  $g_c$  back to the register and repeating step (i) with  $g \mapsto g + 1$ .

Thus, any graph of  $g = n$  vertices can be generated in at most  $O(2n)$  uses of the EB.

## 4. Implementations

### 4.1. Optical lattice realization

The physical basis for the implementation of this scheme which we focus on is an optical lattice of ultracold bosonic atoms [26]. In an optical lattice, neutral atoms are trapped due to the optical dipole force in the intensity maxima (or minima) of a far-off resonance standing wave light-field formed from counter-propagating lasers. We consider atoms possessing two long-lived internal (hyperfine) states  $|a\rangle$  and  $|b\rangle$  which are trapped by two such optical lattices of different polarizations. For sufficiently low temperatures and deep lattices, the atoms become restricted to the lowest Bloch band and their dynamical evolution over a system of  $N$  sites is described by a two-species Bose–Hubbard model (BHM) given by [27]

$$H = \sum_{n=1}^N \left( \frac{U_n^a}{2} a_n^{\dagger 2} a_n^2 + \frac{U_n^b}{2} b_n^{\dagger 2} b_n^2 + U_n^{ab} a_n^{\dagger} a_n b_n^{\dagger} b_n \right) - \sum_{n=1}^{N-1} (t_n^a a_n^{\dagger} a_{n+1} + t_n^b b_n^{\dagger} b_{n+1} + \text{hc}) + H_B, \quad (4)$$

where  $a_n(b_n)$  is the bosonic destruction operator for an  $a(b)$ -atom in the  $n$ th site, and  $H_B = (B/2) \sum_n (a_n^\dagger a_n - b_n^\dagger b_n)$  is the contribution of an external field which we assume to be uniform over the system. The parameters  $t^{a(b)}$  and  $U^{a(b)}$ ,  $U^{ab}$  are the laser-intensity-dependent hopping matrix elements and on-site interactions for atoms in states  $|a\rangle$  ( $|b\rangle$ ) respectively. These parameters will in general have a spatial profile across the lattice. The dynamic controllability and long decoherence times of this system have made it of considerable interest for QIP [28, 29] and for realizing spin models [27, 30].

As outlined in section 3, the scheme requires an initial state with one atom per site (each in a state  $|a\rangle$ ) and single site addressability for manipulations. While the preparation of a high-fidelity initial state could be achieved using the techniques described in [31, 32], single-site addressability remains a challenging technical limitation in optical lattices. However, there are theoretical proposals which offer the potential to overcome this by using ideas such as marker atoms to localize global operations [33], as well as increasing technical improvements in experiments. Hence it does not seem unrealistic to assume that single-site addressability will become possible in the near future.

Initially, we take the lattice as being sufficiently deep to prohibit hopping in all directions. A chain of sites from the commensurately filled lattice is then selected to be the register of non-interacting qubits, and an adjacent chain becomes the EB. Addressability is exploited to engineer a spatially dependent intensity profile along the EB chain which activates hopping exclusively along this chain. The transfer process between the register and EB is accomplished by again using addressability to localize Raman-induced hopping [26] between two adjacent register and EB sites and so implement a swap gate, as described in detail in [28], on a timescale sufficiently faster than  $\tau$ .

For the non-zero hopping within the EB chain, we focus on the two-species BHM in the limit of large interactions,  $U^a, U^b, U^{ab} \gg t^a, t^b$ , which energetically prohibit the multiple occupancy of any site. The hopping can be then treated perturbatively and to lowest order, for an initial Mott insulating state with commensurate filling of one atom per lattice site, the effective Hamiltonian is found to be [27]

$$H_s = \sum_{n=1}^N \lambda_n^z \sigma_n^z + \sum_{n=1}^{N-1} \lambda_n^{zz} \sigma_n^z \sigma_{n+1}^z - \lambda_n^{xy} (\sigma_n^x \sigma_{n+1}^x + \sigma_n^y \sigma_{n+1}^y). \quad (5)$$

Hence we obtain the anisotropic Heisenberg spin model in the optical lattice, with the correspondence  $|a\rangle \equiv |\uparrow\rangle$  and  $|b\rangle \equiv |\downarrow\rangle$  at each site. The corresponding Pauli operators are then  $\sigma_n^z = a_n^\dagger a_n - b_n^\dagger b_n$ ,  $\sigma_n^x = a_n^\dagger b_n + b_n^\dagger a_n$ ,  $\sigma_n^y = -i(a_n^\dagger b_n - b_n^\dagger a_n)$ , while the couplings are given by

$$\lambda_n^z = 4 \left( \frac{t_n^{a2}}{U_n^a} - \frac{t_n^{b2}}{U_n^b} \right) + \frac{B}{2}, \quad \lambda_n^{zz} = \frac{t_n^{a2} + t_n^{b2}}{2U_n^{ab}} - \frac{t_n^{a2}}{U_n^a} - \frac{t_n^{b2}}{U_n^b}, \quad \lambda_n^{xy} = \frac{t_n^a t_n^b}{U_n^{ab}}. \quad (6)$$

The construction of the EB requires the optical lattice parameters to be engineered such that  $U_n^a = U_n^b = 2U_n^{ab}$  and  $t_n^a = t_n^b$ , thereby ensuring that  $\lambda_n^{zz} = 0$ ,  $\lambda_n^z = B/2$ , and that  $H_s$  reduces to the pure XY spin-chain Hamiltonian  $H_{xy}$ .

The spatial dependence of the two-species BHM model parameters arises due to some appropriately configured laser-intensity profile along the system. Since the on-site interactions have a weak dependence on the laser intensity, in contrast to hopping matrix elements which



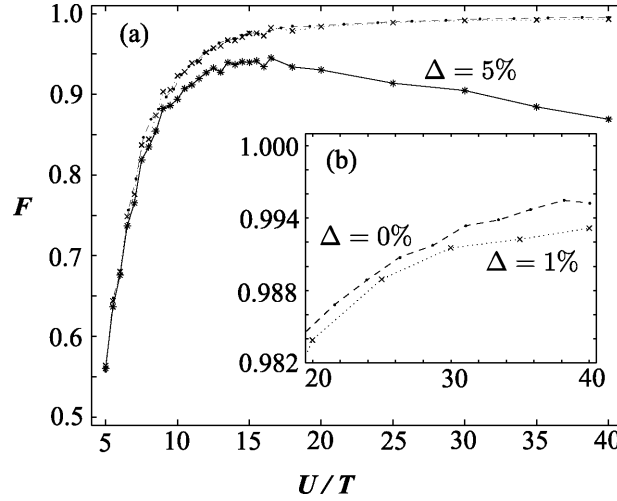


**Figure 4.** (a) The fidelity  $F$  of the effective  $XY$  spin chain implemented by the two-species BHM with the ratio  $U/T$ , for no noise  $\Delta = 0\%$  ( $\cdot$ ),  $\Delta = 1\%$  ( $\times$ ) and  $\Delta = 5\%$  ( $*$ ). (b) A close-up of (a). The solid, dashed and dotted lines are drawn to guide the eye.

have an exponential dependence [26], only hopping is assumed to be spatially dependent over the system. Specifically, we take  $t_n^a = t_n^b = T\sqrt{\alpha_n}$ , where the spatial dependence is again contained in the profile  $\alpha_n$ , and the overall scaling is given by a constant  $T$  such that  $\max(t_n^{a(b)}) \leq T$ . The interaction energies are constant over the system and defined as  $U^a = U^b = 2U^{ab} = U$ . To first order in  $T/U$ , the dynamics of the optical lattice reduces to an  $XY$  spin chain with couplings  $\lambda_n^{xy} = (2T^2/U)\alpha_n$ . The profile  $\alpha_n$  must then have the spatial dependence introduced earlier in section 2 enabling the effective non-interacting fermionic lattice resulting from this  $XY$  spin chain to undergo mirror-inversion. This dynamical evolution will proceed exactly in the ideal limit where  $U/T \gg 1$ . The graph states generated with this implementation could then be used for one-way quantum computation if single site imaging was available, or alternatively the multiqubit entanglement could be diagnosed with the procedure described in [34].

#### 4.2. Optical lattice imperfections

We consider some dominant sources of imperfections within the optical lattice implementation of the EB. In particular, we investigate the fidelity of the two-species BHM to spin-chain mapping introduced earlier, for finite  $U/T$ . For a system of size  $N = 6$  initialized in a product state  $|+\rangle \otimes |0\rangle^{\otimes 4} \otimes |+\rangle$ , we compute the exact time-evolution of the two-species BHM, using the time-evolving block decimation (TEBD) algorithm [35, 36], for varying  $U/T$  over the appropriate inversion time  $\tau$ . Using the effective two-spin density matrix for the end sites, the fidelity  $F$  was computed with the state  $|G_2\rangle$  obtained from a perfectly implemented  $XY$  chain. The simulation results in figure 4(a) demonstrate that, as expected, the fidelity increases with  $U/T$ . Given that  $\tau = UN\pi/16T^2$ , the increasing fidelity, induced by deepening the lattice, comes at the cost of longer inversion times. However, figure 4(b) shows that  $F > 0.99$  even at a moderate ratio of  $U/T = 26$ , and we found this curve to be largely independent of  $N$  for  $N \sim O(10)$  tested. At this depth, a  $\lambda = 514$  nm optical lattice of  $^{23}\text{Na}$  atoms has  $\tau = 9.3$  ms, while a  $\lambda = 826$  nm optical

lattice of  $^{87}\text{Rb}$  atoms has  $\tau = 79$  ms. These are fast enough for multiple EB inversions to occur within the decoherence time of the system, which is typically of the order of a second [37, 38].

We also investigate the effect of jitter in the lattice laser intensities. For  $^{87}\text{Rb}$  the laser intensities  $I_a$  and  $I_b$  of the  $a$  and  $b$  lattices were taken as varying independently according to some Wiener noise  $dW_{a(b)}(t)$  with variance  $\Delta^2$ :  $I_{a(b)}(t) = I_0 + dW_{a(b)}(t)$ , where  $I_0$  is the ideal laser intensity. Such laser fluctuations are then nonlinearly related to the corresponding fluctuations in the hopping  $t_n^{a(b)}$  and on-site interaction  $U^{a(b)}$ ,  $U^{ab}$  matrix elements of the two-species BHM [26]. We assume a simplified version of this noise in which the intensity fluctuations alter, according to these nonlinear relations, the hopping and interaction scalings  $T$  and  $U$  contained within the overall scaling  $W = 4T^2/U$  of  $j_n$ , but not the spatial profile  $\alpha_n$ . Despite this restriction, this noise causes fluctuations in the inversion time  $\tau$  during the dynamical evolution, and also breaks the symmetry required to ensure that no  $\sigma_n^z \sigma_{n+1}^z$  or spatially varying  $\sigma_n^z$  contributions occur. In figure 4(a) the fidelity curves are plotted for  $\Delta = 1$  and 5% of  $I_0$ . For  $\Delta = 5\%$  the fidelity is seen to drop-off in deeper lattices due to the cumulative effect of noise over longer inversion times. Crucially, the fidelity curve suffers only a minimal reduction due to  $\Delta = 1\%$  noise, as in figure 4(b), and this represents a realistic value for the experimental stabilization of the laser intensity.

### 4.3. Alternative implementations

Finally, we note that the scheme described in section 3 could be implemented in any physical system where the entangling operation  $\mathcal{C}$  is available. Specifically the architecture composed of a register and EB considered here could in principle be implemented wherever two adjacent engineered spin chains are realizable. This requirement is particularly well suited to solid-state systems such as arrays of quantum dots with one electron per dot in an external magnetic field [39, 40]. Here the qubit is encoded in the spin degree of freedom of the electron and the dynamical evolution is described by a standard Heisenberg Hamiltonian. The presence of  $\sigma_n^z \sigma_{n+1}^z$  terms in this Hamiltonian can be compensated by an appropriate spatially varying external magnetic field [16], while the angular momentum coupling profile can then be produced by controlling the external voltage applied to the gates defining the tunnelling barriers between the dots. However, such an implementation is currently limited by the small number of solid-state qubits realizable.

Another possibility is trapped ions [41]. A scheme for generating GHZ-type states over a chain of many ions has been proposed [42] and experimentally realized for four qubits [4]. Although implemented by different means, the entangling procedure in [42] is locally equivalent to the entangling operation  $\mathcal{C}$  when it is applied globally to the entire register. Permitting single-ion addressability, which has also been experimentally demonstrated [43], allows universal two-qubit quantum gates to be implemented by the same method [44], and additionally, by addressing many ions,  $\mathcal{C}$  can be applied to any subset of qubits. Thus the entangling operation constructed above for optical lattices via the EB is also realizable in ion-trap systems via the collective vibrational degrees of freedom of the ions.

## 5. Conclusions

We have shown how arbitrary graph states can be generated efficiently by using an EB whose dynamical evolution corresponds to a non-interacting fermionic system undergoing mirror-inversion. By utilizing an EB which is fixed and always on the dynamical control required

for QIP, tasks can be reduced to single-qubit operations. Here an implementation of this scheme using an optical lattice of neutral atoms was considered in detail. The fidelity of the optical lattice proposal was examined not only for the depth ratio  $U/T$ , but also in the presence of noise, and found to be both realistic and robust. We have also briefly noted the suitability of the scheme to other physical systems.

## Acknowledgments

This work was supported by the EPSRC (UK) through the QIP IRC ([www.qipirc.org](http://www.qipirc.org)) (GR/S82176/01) and the project EP/C51933/1. SRC and DJ thank Peter Zoller and Hans Briegel for stimulating discussions. CMA thanks Marc Hein for insightful discussions on graph states and is supported by the Fundação para a Ciência e Tecnologia (Portugal).

## References

- [1] Mandel O, Greiner M, Widera A, Rom T, Hänsch T W and Bloch I 2003 *Nature* **425** 937
- [2] Walther P, Pan J W, Aspelmeyer M, Ursin R, Gasparoni S and Zeilinger A 2004 *Nature* **429** 158
- [3] Walther P, Resch K J, Rudolph T, Schenck E, Weinfurter H, Vedral V, Aspelmeyer M and Zeilinger A 2005 *Nature* **434** 169
- [4] Sackett C A, Kielpinski D, King B E, Langer C, Meyer V, Myatt C J, Rowe M, Turchette Q A, Itan W M, Wineland D J and Monroe C 2000 *Nature* **404** 256
- [5] Rauschenbeutel A, Nogues G, Osnaghi S, Bertet P, Brune M, Raimond J M and Haroche S 2000 *Science* **288** 2024
- [6] Hein M, Eisert J and Briegel H J 2004 *Phys. Rev. A* **69** 062311
- [7] Briegel H J and Raussendorf R 2001 *Phys. Rev. Lett.* **86** 910
- [8] Gottesman D 1997 *PhD Thesis* CalTech, Pasadena
- [9] Steane A M 1996 *Phys. Rev. Lett.* **77** 793
- [10] Raussendorf R and Briegel H J 2001 *Phys. Rev. Lett.* **86** 5188
- [11] Raussendorf R, Browne D E and Briegel H J 2003 *Phys. Rev. A* **68** 022312
- [12] Browne D E and Rudolph T 2004 *Preprint* quant-ph/0405157
- [13] Barrett S D and Kok P 2004 *Preprint* quant-ph/0408040
- [14] Bravyi S B and Kitaev A Y 2002 *Ann. Phys.* **298** 210
- [15] Sachdev S 2001 *Quantum Phase Transitions* (Cambridge: Cambridge University Press)
- [16] Christandl M, Datta N, Ekert A and Landahl A J 2004 *Phys. Rev. Lett.* **92** 187902
- [17] Zanardi P 2002 *Phys. Rev. A* **65** 042101
- [18] Zanardi P and Wang X 2002 *J. Phys. A: Math. Gen.* **35** 7947
- [19] Wu L A and Lidar D A 2002 *J. Math. Phys.* **43** 4506
- [20] Vedral V 2003 *Central Eur. J. Phys.* **1** 289
- [21] Yung M H and Bose S 2004 *Quantum Inform. Comput.* **4** 174
- [22] Yung M H and Bose S 2005 *Phys. Rev. A* **71** 032310
- [23] Recati A, Fedichev P O, Zwerger W, von Delft J and Zoller P 2005 *Phys. Rev. Lett.* **94** 040404
- [24] Calarco T, Hinds E A, Jaksch D, Schmiedmayer J, Cirac J I and Zoller P 2000 *Fortschr. Phys.* **48** 945
- [25] Paredes B, Widera A, Murg V, Mandel O, Fölling S, Cirac J I, Shlyapnikov G V, Hänsch T W and Bloch I 2004 *Nature* **429** 277
- [26] Jaksch D, Bruder C, Cirac J I, Gardiner C W and Zoller P 1998 *Phys. Rev. Lett.* **81** 3108
- [27] Duan L M, Demler E and Lukin M D 2003 *Phys. Rev. Lett.* **91** 090402
- [28] Pachos J K and Knight P L 2003 *Phys. Rev. Lett.* **91** 107902
- [29] Jaksch D and Zoller P 2004 *Ann. Phys.* **315** 52

- [30] García-Ripoll J J and Cirac J I 2003 *New J. Phys.* **5** 76
- [31] Griessner A, Daley A J, Jaksch J and Zoller P 2005 *Preprint* quant-ph/0502171
- [32] Rabl P, Daley A J, Fedichev P O, Cirac J I and Zoller P 2003 *Phys. Rev. Lett.* **91** 110403
- [33] Calarco T, Dorner U, Julienne P, Williams C and Zoller P 2004 *Phys. Rev. A* **70** 012306
- [34] Moura Alves C and Jaksch D 2004 *Phys. Rev. Lett.* **93** 110501
- [35] Vidal G 2003 *Phys. Rev. Lett.* **91** 147902
- [36] Vidal G 2004 *Phys. Rev. Lett.* **93** 040502
- [37] Greiner M, Mandel O, Esslinger T, Hänsch T W and Bloch I 2002 *Nature* **415** 39
- [38] Hensinger W K *et al* 2001 *Nature* **412** 52
- [39] Golovach V N and Loss D 2002 *Semicond. Sci. Technol.* **17** 355
- [40] Pashkin Y A, Yamamoto T, Astafiev O, Nakamura Y, Averin D V and Tsai J S 2003 *Nature* **421** 823
- [41] Cirac J I and Zoller P 1995 *Phys. Rev. Lett.* **74** 4091
- [42] Mølmer K and Sørensen S 1999 *Phys. Rev. Lett.* **82** 1835
- [43] Roos C, Riebe M, Häffner H, Hänsel W, Benhelm J, Lancaster G P T, Becher C, Schmidt-Kaler F and Blatt R 2004 *Science* **304** 1478
- [44] Sørensen S and Mølmer K 1999 *Phys. Rev. Lett.* **82** 1971